

Optimal Excess Noise Reduction in Thin Heterojunction $\text{Al}_{0.6}\text{Ga}_{0.4}\text{As}$ –GaAs Avalanche Photodiodes

Oh-Hyun Kwon, Majeed M. Hayat, *Senior Member, IEEE*, Shuling Wang, Joe C. Campbell, *Fellow, IEEE*, Archie Holmes, Jr., *Member, IEEE*, Yi Pan, *Senior Member, IEEE*, Bahaa E. A. Saleh, *Fellow, IEEE*, and Malvin C. Teich, *Fellow, IEEE*

Abstract—It has been recently found that the initial-energy effect, which is associated with the finite initial energy of carriers entering the multiplication region of an avalanche photodiode (APD), can be tailored to reduce the excess noise well beyond the previously known limits for thin APDs. However, the control of the initial energy of injected carriers can be difficult in practice for an APD with a single multiplication layer. In this paper, the dead-space multiplication recurrence theory is used to show that the low noise characteristics associated with the initial-energy effect can be achieved by utilizing a two-layer multiplication region. As an example, a high bandgap $\text{Al}_{0.6}\text{Ga}_{0.4}\text{As}$ material, termed the energy-buildup layer, is used to elevate the energy of injected carriers without incurring significant multiplication events, while a second GaAs layer with a lower bandgap energy is used as the primary carrier multiplication layer. Computations show that devices can be optimally designed through judicious choice of the charge-layer width to produce excess noise factor levels that are comparable to those corresponding to homojunction APDs benefiting from a maximal initial-energy effect. A structure is presented to achieve precisely that.

Index Terms— $\text{Al}_{0.6}\text{Ga}_{0.4}\text{As}$, avalanche photodiodes, dead space, excess noise factor, GaAs, heterostructure APDs, impact ionization, initial-energy effect, ionization threshold energy, optimization.

I. INTRODUCTION

IT IS KNOWN that the excess noise factor in avalanche photodiodes (APDs), which is a measure of gain uncertainty in such devices, can be significantly reduced by decreasing the thickness of the avalanche region. It is also well known that the dead space, which is the minimum distance that a carrier must travel before acquiring sufficient energy enabling it to impact ionize, is the primary cause of this noise reduction.

Manuscript received March 5, 2003; revised May 12, 2003. This work was supported by the National Science Foundation.

M. M. Hayat and O.-H. Kwon are with the Department of Electrical and Computer Engineering, The University of New Mexico, Albuquerque, NM 87131–1356 USA (e-mail: hayat@ece.unm.edu; ohyun@unm.edu).

S. Wang, J. C. Campbell and A. Holmes, Jr., are with the Department of Electrical and Computer Engineering, The University of Texas at Austin, Austin, TX 78712 USA (e-mail: swang2@ece.utexas.edu; jcc@mail.utexas.edu; holmes@mail.utexas.edu).

Y. Pan is with the Department of Computer Science, Georgia State University, Atlanta, GA, 30303 USA (e-mail: pan@cs.gsu.edu).

B. E. A. Saleh and M. C. Teich are with the Department of Electrical and Computer Engineering, Boston University, Boston, MA 02215–2421 USA (e-mail: besaleh@bu.edu; teich@bu.edu).

Digital Object Identifier 10.1109/JQE.2003.817671

Lately, a new class of heterostructure APDs [1], [2] has been demonstrated to exhibit excess noise factors that are well below the predictions of the dead-space-inclusive multiplication models for thin APDs [3]–[16]. In particular, Yuan *et al.* [1] introduced APDs with an “impact-ionization-engineered” (I^2E) multiplication region and showed a minimum excess noise factor of approximately 2.5 at a gain of 20. The corresponding APD had a multiplication region consisting of three layers: 50-nm-GaAs, 85-nm- $\text{Al}_{0.6}\text{Ga}_{0.4}\text{As}$, and 50-nm-GaAs layers. This is a remarkable noise performance as it surpasses all previous experimental results and analytical predictions. For example, theoretical models predict an excess noise factor of approximately 6.5 (at a gain of 20) for a 100-nm homojunction GaAs APD [17]. The original idea of the I^2E structure was to sandwich a separation layer with high ionization threshold energy between two thin layers with low ionization threshold energy. Low multiplication noise is achieved by means of localizing the location of impact ionizations: Due to carrier-energy considerations, electron ionizations are forced to occur in one of the low-threshold layers while hole ionizations occur in the opposite low-threshold layer, and at the same time, ionizations are highly suppressed in the high-threshold separation layer [1]. Subsequently, variants of I^2E APDs were introduced. For example, Wang *et al.* [2] demonstrated an excess noise factor of 3.8 at a gain of 20 using a four-layer graded I^2E multiplication region consisting of 50-nm-GaAs, 10-nm- $\text{Al}_{0.2}\text{Ga}_{0.8}\text{As}$, 30-nm- $\text{Al}_{0.4}\text{Ga}_{0.6}\text{As}$, and 50-nm- $\text{Al}_{0.6}\text{Ga}_{0.4}\text{As}$ layers. The localization of impact ionization in I^2E structures has been recently confirmed by Monte-Carlo studies [18], [19].

More recently, it has been shown that noise reduction beyond the traditional dead-space-based limit is indeed possible through a mechanism called the initial-energy effect [17], [20]. In certain structures, injected carriers enter the multiplication region with substantial kinetic energy. This energy buildup occurs, for example, when a carrier experiences a sharp electric-field gradient in the doped region just before the multiplication layer. Such an initial energy serves to reduce the initial dead space associated with the injected avalanche-initiating carrier. This will, in turn, enhance the likelihood that the injected carrier impact ionizes near the edge of the multiplication region. The reduction in the excess noise factor results from the *strong localization of the first impact ionization event at the beginning of the multiplication region*, an event that is akin to having two injected carriers per absorbed photon [17]. For example, it has been shown

that in thin devices (e.g., < 200 nm) for which injected carriers accumulate a substantial initial energy (close to the ionization threshold energy), a reduction up to 45% in the excess noise factor is achievable in comparison to devices for which the initial-energy effect is absent [17]. Moreover, it has been theoretically shown that as devices become thinner, the initial-energy effect can become more pronounced [17].

Similar ionization localization effects have also been observed in other structures. Herbert *et al.* [21] demonstrated that a Si-SiGe MQW APD exhibits lower multiplication noise than a Si APD. The noise reduction was attributable to the fact that carriers are first heated in the Si layers before they ionize in the thin SiGe layers. (They even showed lower noise in a hetero-*nipi* structure by heating the electrons and cooling the holes before they enter the SiGe layers.) Indeed, the heating effect on both the MQW and the hetero-*nipi* considered by Herbert *et al.* is akin to the initial-energy effect considered in this paper in that electrons are first energized (heated) before entering the “multiplication layer,” which results in a reduction in the multiplication noise. Thus, in the context of our paper, each Si layer serves as an “energy-buildup” layer whereas each SiGe layer serves as a “multiplication layer.” In this paper, however, we explicitly draw the connection between the energy buildup (or heating) of a carrier in the high bandgap material and the reduction of its first dead space in the low bandgap multiplication layer. Moreover, we definitively establish the reduction of the multiplication noise as a result of miniaturizing the first dead space.

Plimmer *et al.* [22] also demonstrated noise reduction in p^+-n junctions as a result of injecting carriers into a multiplication region exhibiting a steep downward electric-field gradient. We believe that such a noise reduction is also attributable to the reduction in the initial dead space of injected carriers. Namely, carriers that are injected into the multiplication region will initially experience a minimal initial dead space due to the field gradient.

To date, means for accurately controlling the electric field in the doped region just outside the multiplication layer (near the boundary of the doped and intrinsic layers) during the fabrication process are not available. As a result, the initial-energy effect may vary significantly from one sample to another, making reliable production of such low-noise APDs difficult. Fortunately, an alternate method has been proposed to bring about the initial-energy effect [18], [20] without relying on the presence of a sharp field gradient in the doped region just before the multiplication region. The alternative technique relies on the use of a two-layer heterostructure multiplication region for which a high-field and high-bandgap intrinsic layer, called the energy-buildup layer, is dedicated to elevating the energy of carriers without incurring significant ionization within the layer, while an adjacent high-field and low-bandgap intrinsic layer is used to host the bulk of the impact ionizations. In this way, *energized* carriers are injected into the low-ionization-threshold layer having a high probability of bypassing the initial dead space entirely and impact ionizing immediately. In this paper, we present a noise analysis for such heterojunction multiplication-region APDs using a recently developed analytical model that incorporates the initial-energy

effect in heterostructure APDs [17]. The analytical model also enables us to design optimized APDs for which the width of the layers (the energy-buildup layer, in particular) are judiciously selected to minimize the excess noise factor.

In summary, the ionization localization effect near the edge of the multiplication region, as described above, is attributed to the combination of: 1) the energy that injected carriers build up prior to entering the low-bandgap multiplication layer and 2) the drop in the ionization threshold energy from high-bandgap energy-buildup layer to the low-bandgap multiplication layer. These two factors collectively lead to a reduced initial dead space for each injected carrier and, thus, a reduced multiplication noise. We wish to emphasize, however, that the noise reduction mechanism described in this paper is *different* from that postulated by Williams *et al.* [23], in which an enhancement in the ionization coefficients is assumed at the $\text{Al}_{0.6}\text{Ga}_{0.4}\text{As}$ -GaAs boundary. To the contrary, we do not assume any accentuation in the ionization probability as a result of the band-edge discontinuity at the hetero-interface. In fact, several Monte-Carlo studies on $\text{Al}_{0.6}\text{Ga}_{0.4}\text{As}$ -GaAs multilayers showed that band-edge discontinuities in multilayer structures appeared to offer no ionization-coefficient enhancement due to carrier energy losses brought about by phonon scattering [24], [25].

II. NOISE REDUCTION DUE TO THE INITIAL-ENERGY EFFECT

The noise characteristics of homojunction avalanche photodiodes can be modeled using the dead-space multiplication theory (DSMT) [3]–[5], [8], [10], which has been recently generalized to incorporate the initial-energy effect [17]. We call this generalized model the modified dead-space multiplication theory (MDSMT). The key parameters needed by the MDSMT are the material-specific ionization coefficients for electrons and holes, which are independent of the multiplication-layer width, the electron and hole ionization threshold energies, and the initial energy that injected carriers possess. The ionization coefficient for enabled electrons (those that have traveled the required dead space) is given by

$$\alpha(x) = A \exp \left[- \left(\frac{\mathcal{E}_c}{\mathcal{E}(x)} \right)^m \right] \quad (1)$$

where A , \mathcal{E}_c , and m are parameters obtained from noise-versus-gain data [7], [8], [14], and $\mathcal{E}(x)$ is the applied electric field. (A similar expression is available for enabled holes.) These ionization coefficients are used in conjunction with the dead-space profile and the initial energy of injected carriers to yield the position-dependent impact ionization probability density function (pdf) for carriers with injected (parent) and offspring carriers having different densities since only injected carriers have an initial energy. These pdfs are then used in the recurrence equations for carrier multiplication [17] to yield the gain and the excess noise factor. The details of the MDSMT can be found in [17]. In this paper, the parameters for the ionization coefficients and threshold energies for GaAs and $\text{Al}_{0.6}\text{Ga}_{0.4}\text{As}$ are taken, respectively, from Saleh *et al.* [8] and Plimmer *et al.* [14].

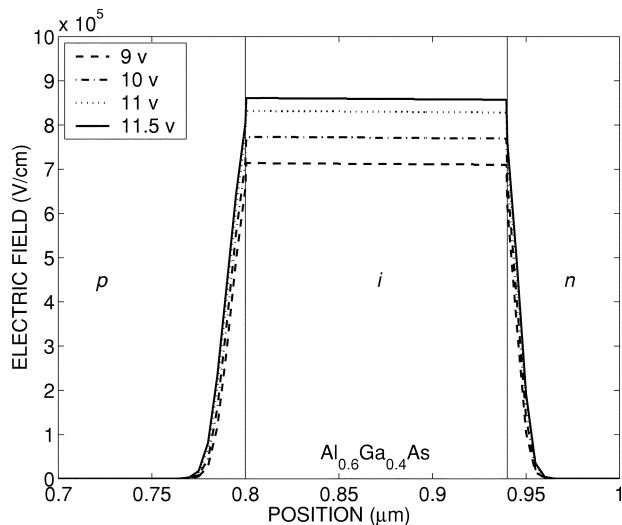


Fig. 1. Electric-field profile for an $\text{Al}_{0.6}\text{Ga}_{0.4}\text{As}$ homojunction APD with a 140-nm multiplication layer. The profiles are parameterized by the applied voltages.

A. Experimental Validation of the MDSMT Model

In Section III, we will synthesize the initial-energy effect through the use of the energy-buildup layer and use the MDSMT to optimize the design for minimum noise. But before that, we will demonstrate the validity of the MDSMT model and show its ability to predict the low-noise characteristics of an APD for which injected carriers have a finite initial energy. We consider an $\text{Al}_{0.6}\text{Ga}_{0.4}\text{As}$ homojunction APD that was recently fabricated and tested at the Microelectronics Research Center at the University of Texas in Austin. The device has a single multiplication layer whose width is 140 nm. Fig. 1 shows the electric field distribution in the APD showing the sharp field gradient in the p region near the edge of the i (multiplication) layer. The initial energy buildup can be computed from the electric field distribution in the p layer. For example at a gain of 20, the energized electrons start the multiplication process with an initial energy of 0.9 eV, which is approximately 26% of the ionization threshold energy for $\text{Al}_{0.6}\text{Ga}_{0.4}\text{As}$ for which $E_{\text{th},\text{Al}_{0.6}\text{Ga}_{0.4}\text{As}} = 3.4$ eV [14]. Due to this initial energy, the first dead space is also reduced by approximately 26%. The solid curve in Fig. 2 is the excess-noise-factor prediction of the device with the initial energy taken into account. As can be seen from the figure, the results are in excellent agreement with the measurement. Furthermore, our calculations show that if the device were fabricated such that electrons would build up 100% of ionization threshold energy before entering the multiplication layer, then the noise would be additionally reduced by 35% at a gain of 20 (dashed curve). Note that the actual noise for this device would have been considerably overestimated had we neglected the initial energy of injected carriers (dotted curve).

B. Noise Reduction due to the Initial-Energy Effect

Next, we consider the noise characteristics of heterostructure APDs that exhibit behavior similar to that of the initial-energy effect. In particular, we consider a heterostructure device with a multiplication region consisting of two intrinsic layers, $\text{Al}_{0.6}\text{Ga}_{0.4}\text{As}$ and GaAs, for which carriers are injected into the

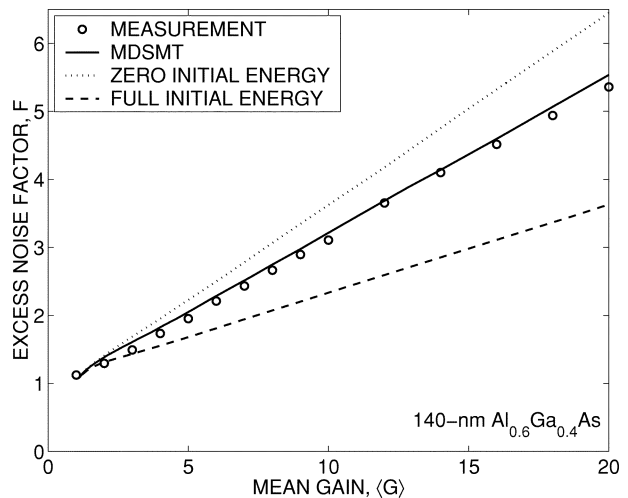


Fig. 2. Excess noise factor F versus the mean gain $\langle G \rangle$ for different initial-energy scenarios. The theoretical (MDSMT) prediction which includes the actual initial energy is in excellent agreement with experiment.

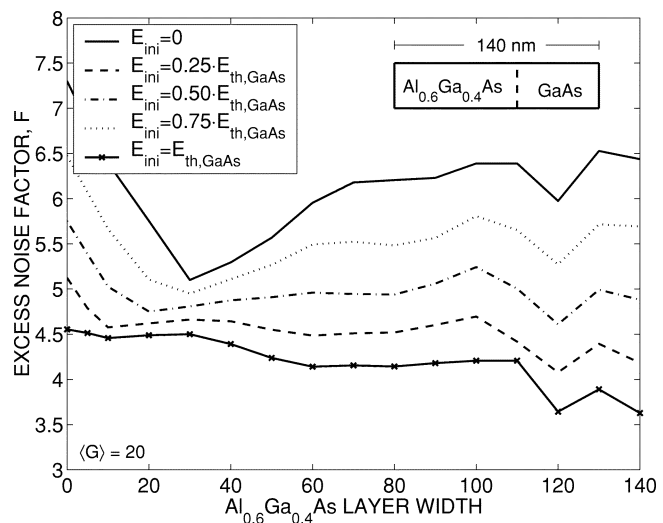


Fig. 3. Dependence of the excess noise factor in $\text{Al}_{0.6}\text{Ga}_{0.4}\text{As}$ /GaAs heterostructure APDs on the width of the $\text{Al}_{0.6}\text{Ga}_{0.4}\text{As}$ energy-buildup layer. The plots are parameterized by different initial-energy levels of the carriers that are injected into the $\text{Al}_{0.6}\text{Ga}_{0.4}\text{As}$ layer. The initial-energy values are taken relative to the ionization threshold energy of GaAs.

$\text{Al}_{0.6}\text{Ga}_{0.4}\text{As}$ layer. In the calculations, the excess noise factor is computed for different widths of the $\text{Al}_{0.6}\text{Ga}_{0.4}\text{As}$ layer while the total multiplication layer width was fixed at 140 nm and the mean gain was fixed at 20. We will also consider varying the initial energy, E_{ini} , of the carriers that enter the $\text{Al}_{0.6}\text{Ga}_{0.4}\text{As}$ layer. This is an important issue to examine since it is generally hard to reliably reproduce devices with prescribed field gradients (in the p region near the i -layer boundary).

The results are shown in Fig. 3. The solid curve represents the theoretical excess noise factor with zero initial energy (i.e., normal initial dead space) and the solid curve with x-marks represents the excess noise factor with full initial energy (i.e., zero initial dead space). The figure also shows the intermediate cases of the initial energy for carriers that enter the $\text{Al}_{0.6}\text{Ga}_{0.4}\text{As}$ layer. Note that the lowest noise, for the case $E_{\text{ini}} = 0$, is observed when the width of the $\text{Al}_{0.6}\text{Ga}_{0.4}\text{As}$ layer is 30 nm. The reason for this is that electrons build up energy in the range between $E_{\text{th},\text{GaAs}} = 1.90$ eV [8] and $E_{\text{th},\text{Al}_{0.6}\text{Ga}_{0.4}\text{As}} = 3.4$ eV

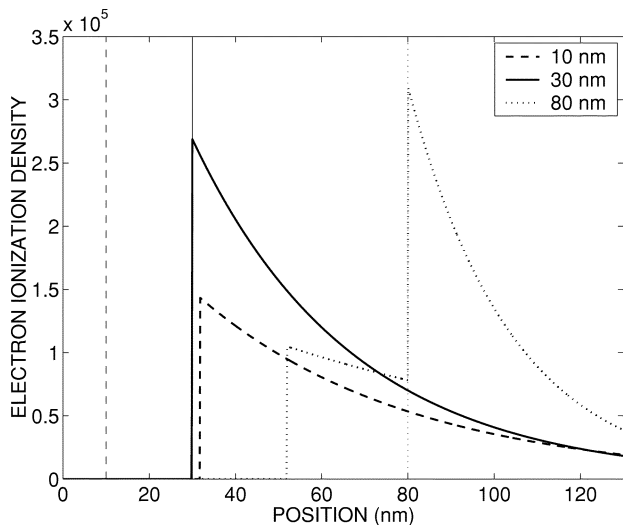


Fig. 4. Electron ionization pdf. Low excess noise necessitates a peak at the boundary layer (30-nm, solid curve). The shorter (dashed curve) and longer (dotted curve) $\text{Al}_{0.6}\text{Ga}_{0.4}\text{As}$ -layer widths result in a spread of pdf and hence the ionization events. Vertical curves represent the physical layer boundary in each case.

as they travel approximately 30-nm deep into the $\text{Al}_{0.6}\text{Ga}_{0.4}\text{As}$ layer. As a result, electrons arrive at the boundary without ionizing and with an energy approximately equal to the ionization threshold energy for $\text{Al}_{0.6}\text{Ga}_{0.4}\text{As}$. Now, as soon as these electrons cross the boundary, they experience a sudden drop in the ionization threshold energy to that of GaAs. Since they have already acquired an energy in excess of the required 1.90 eV, they will be ready to impact ionize immediately after crossing the boundary.

This can be seen from the electron ionization pdf plot shown in Fig. 4. When the $\text{Al}_{0.6}\text{Ga}_{0.4}\text{As}$ layer is 30 nm (solid curve), there is a strong peak in the ionization density at 30 nm. This quasi localization of the initial impact ionization is responsible of the noise reduction. On the other hand, for longer widths of the $\text{Al}_{0.6}\text{Ga}_{0.4}\text{As}$ layer, 80 nm for example (dotted curve), electrons acquire sufficient energy for impact ionization within the $\text{Al}_{0.6}\text{Ga}_{0.4}\text{As}$ layer. Consequently, they start impact ionizing before they reach the boundary. There is another strong probability of impact ionization at the boundary at 80 nm. This leads to increased uncertainty of the initial impact ionization and higher excess noise factor. The noise characteristics in this regime is consistent with that of an $\text{Al}_{0.6}\text{Ga}_{0.4}\text{As}$ -GaAs alloy. Finally, for shorter widths of the $\text{Al}_{0.6}\text{Ga}_{0.4}\text{As}$ layer, 10 nm for example (dashed curve), injected electrons do not have sufficient distance to travel in the $\text{Al}_{0.6}\text{Ga}_{0.4}\text{As}$ layer to accumulate energy in excess of the required $E_{\text{th,GaAs}}$. As a result, electrons are not capable of immediate impact ionization at the boundary. They must travel farther into the GaAs layer to acquire sufficient energy and to overcome the residual dead space in the GaAs layer. As shown in Fig. 4, the electron ionization pdf of a short (10-nm) $\text{Al}_{0.6}\text{Ga}_{0.4}\text{As}$ -layer (dashed curve) is flattened and spread out, causing a loss of the localization effect.

It is interesting to note from Fig. 3 that the noise is also reduced when the width of the $\text{Al}_{0.6}\text{Ga}_{0.4}\text{As}$ layer is approximately 120 nm. In this case, the electrons that are generated in the GaAs layer cannot acquire sufficient energy to cause fur-

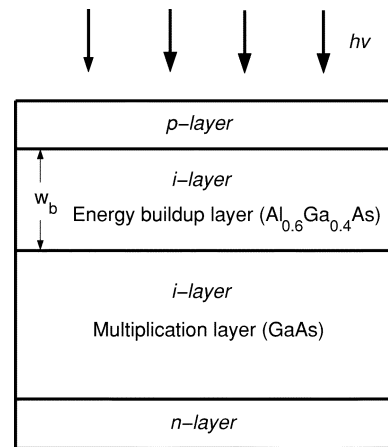


Fig. 5. Schematic of the proposed heterostructure APD. The energy buildup layer is where electrons accumulate energy without initiating the multiplication process. Its width, w_b , plays the key role in reducing the excess noise factor.

ther ionizations. Thus, the contribution of the GaAs layer to impact ionization is partially hampered. This effect causes the $\text{Al}_{0.6}\text{Ga}_{0.4}\text{As}$ -GaAs heterostructure to behave, more or less, like a 120-nm $\text{Al}_{0.6}\text{Ga}_{0.4}\text{As}$ homostructure, which inherently has low noise. As the width of the $\text{Al}_{0.6}\text{Ga}_{0.4}\text{As}$ increases beyond 120 nm, the APD continues to behave like a homostructure, but with a thickness that is greater than 120 nm which, as expected, will cause the noise to increase.

In summary, for a given initial energy of the injected electrons, the heterostructure APD yields the best noise performance if the $\text{Al}_{0.6}\text{Ga}_{0.4}\text{As}$ layer is either 30 or 120 nm wide. As seen in Fig. 3, the 120-nm- $\text{Al}_{0.6}\text{Ga}_{0.4}\text{As}$ /20-nm-GaAs combination may result in the least excess noise factor if the device allows injected electrons to build up full initial energy (in excess of the ionization threshold of $\text{Al}_{0.6}\text{Ga}_{0.4}\text{As}$), which may be impractical. Otherwise, the excess noise factor would be high if the initial energy is low. On the other hand, a 30-nm- $\text{Al}_{0.6}\text{Ga}_{0.4}\text{As}$ /110-nm-GaAs combination yields a reasonably low excess noise factor but with the added advantage of being less sensitive to the initial energy. As can be seen from the vertical extent of the curves in Fig. 3, the excess-noise-factor uncertainty (due to initial-energy uncertainty) for the 30-nm- $\text{Al}_{0.6}\text{Ga}_{0.4}\text{As}$ /110-nm-GaAs combination is $\Delta F = 0.7$, while the uncertainty for the 120-nm- $\text{Al}_{0.6}\text{Ga}_{0.4}\text{As}$ /20-nm-GaAs combination is $\Delta F = 2.3$.

It must be pointed out that if the p and n regions are included in the analysis of multiplication, as part of the multiplication region (instead of only considering the i layers), then the initial-energy effect will be automatically accounted for by the dead space through the strong modulation of the electric field near the i - p and n - i boundaries. However, if only the intrinsic layers are considered as the multiplication region, the initial-energy effect must be accounted for separately, as above.

III. DESIGN CONSIDERATIONS

In the proposed heterostructure APD, shown in Fig. 5, an $\text{Al}_{0.6}\text{Ga}_{0.4}\text{As}$ energy-buildup layer is inserted between the p layer and the GaAs multiplication layer. The energy-buildup layer is intrinsic so as to benefit from the presence of a high

electric field. If the width of the energy-buildup layer is carefully designed, carriers that are injected into the energy-buildup layer (possibly with an unknown initial energy) are able to acquire and maintain energy up until entering the GaAs multiplication layer. However, by the time electrons pass the boundary and cross into the GaAs multiplication layer, their acquired energy will exceed the ionization threshold energy of GaAs. Consequently, these energized electrons will become capable of impact ionizing in the GaAs without any significant dead space. Hence, as far as the GaAs multiplication layer is concerned, carriers injected into it have high initial energy and negligible initial dead space, and the initial-energy effect will thus be strongly present.

In general, there is a small possibility of impact ionization for holes that were created in GaAs far away from the boundary. To address the hole ionization issue more concretely, consider one of the configurations that exhibits a minimal excess noise factor (its analysis was not considered in Section II-B), namely, a device with 40-nm- $\text{Al}_{0.6}\text{Ga}_{0.4}\text{As}$ and 200-nm-GaAs layers. The dead space for a hole in the $\text{Al}_{0.6}\text{Ga}_{0.4}\text{As}$ layer is approximately 72 nm (assuming that $E_{\text{th},\text{Al}_{0.6}\text{Ga}_{0.4}\text{As}}$ for the hole is 3.6 eV and the electric field for a gain of 20 is about 500 kV/cm) and 31 nm in GaAs layer (assuming $E_{\text{th},\text{GaAs}} = 1.55$ eV for the holes [8]). Thus, holes born at a distance of 71 nm or less from the outer edge of the $\text{Al}_{0.6}\text{Ga}_{0.4}\text{As}$ energy-buildup layer (i.e., in the GaAs layer and 31 nm from the boundary) are not able to impact ionize in the GaAs layer nor in the $\text{Al}_{0.6}\text{Ga}_{0.4}\text{As}$ layer since they cannot overcome the dead space in either layer. However, holes born farther than 71 nm from the outer edge of the $\text{Al}_{0.6}\text{Ga}_{0.4}\text{As}$ energy-buildup layer may impact ionization within the GaAs layer. In such an event, an offspring hole enters the $\text{Al}_{0.6}\text{Ga}_{0.4}\text{As}$ layer with low energy and it will be unlikely for it to further ionize in the $\text{Al}_{0.6}\text{Ga}_{0.4}\text{As}$ layer. Thus, over all, the feedback inflicted by holes is expected to be weakened, which may be a contributing factor in noise reduction.

A. Optimal Width of the Energy-Charge Layer

From the above discussion, it is clear that the width of the energy-buildup layer should be large enough so that photogenerated injected carriers can accumulate energy in excess of the electron ionization threshold energy of the multiplication layer. At the same time, the width should be small enough so that the accumulated energy does not exceed the electron ionization threshold energy of the energy-buildup layer. These requirements can be cast as

$$E_{\text{th,mul}} < E_{\text{tot}} < E_{\text{th,eb}} \quad (2)$$

where $E_{\text{th,mul}}$ is the electron ionization threshold energy of the multiplication layer, $E_{\text{th,eb}}$ is the electron ionization threshold energy of the energy-buildup layer, and E_{tot} is the total energy accumulated in the energy-buildup layer plus the initial energy obtained in p -layer, i.e., $E_{\text{tot}} = E_{\text{ini}} + E_{\text{th,eb}}$, where E_{ini} is the initial energy of electrons injected into the energy-buildup layer. Recall that the initial energy E_{ini} can be computed once the doping profile of the device is determined using the exact electric field distribution along the device. Clearly, the acquired

TABLE I
EXAMPLES OF THE RANGE FOR THE OPTIMUM WIDTH OF THE ENERGY-BUILDUP LAYER FOR DIFFERENT MULTIPLICATION LAYER WIDTHS. THE APPLIED ELECTRIC FIELDS CORRESPOND TO A MEAN GAIN OF 20 FOR EACH DEVICE

width (nm)	\mathcal{E} field (kV/cm)	Optimum width (nm), w_b
50	1000	$19 < w_b < 24$
100	660	$29 < w_b < 36$
150	550	$35 < w_b < 44$
200	490	$39 < w_b < 49$

$$\langle G \rangle = 20$$

energy in the energy-buildup layer depends on the applied electric field

$$E_{\text{th,eb}} = q \int \mathcal{E} dx \quad (3)$$

where the integration is over the energy-buildup layer. For a constant electric field and if we let w_b denote the width of the energy-buildup layer, we will have

$$\frac{E}{q} = \mathcal{E} w_b \quad (4)$$

and

$$E_{\text{th,mul}} < \mathcal{E} w_b < E_{\text{th,eb}} - E_{\text{ini}}. \quad (5)$$

(In (5), all energies are divided by q so that their unit is the electron Volt (eV). Thus, the width of the energy-buildup layer must satisfy

$$\frac{E_{\text{th,mul}}}{\mathcal{E}} < w_b < \frac{E_{\text{th,eb}} - E_{\text{ini}}}{\mathcal{E}}. \quad (6)$$

In the above analysis, we assumed that $E_{\text{th,eb}} > E_{\text{ini}}$, which is consistent with the measurements for which $E_{\text{ini}} < 1$ eV [17]. Since the applied electric field determines the gain of the APD, the allowed range for w_b given by (6) depends upon the desired gain and the required electric field dictated by the gain. Several optimum width ranges for different devices are given in Table I.

Fig. 6 shows the calculated excess noise factor, as a function of the energy-buildup layer width, for a mean gain of 20. Different multiplication-layer (GaAs) widths are considered. The curves clearly verify the optimum width ranges obtained from (6), which was determined solely based on energy considerations. For example, for a 100-nm GaAs-multiplication-layer device (dashed curve), the excess noise factor is lowest when the width of the $\text{Al}_{0.6}\text{Ga}_{0.4}\text{As}$ energy-buildup layer is 29 nm. It should be pointed out that the optimum width turns out to be almost independent of the operational mean gain. For example, a 100-nm GaAs APD requires electric-field values of 630 kV/cm and 660 kV/cm in order to generate mean gain values of 10 and 30, respectively. It turns out that such a 5% variation in the electric field results in a 5% variation in the optimal width of the energy-buildup layer (which is equivalent to approximately 1.5 nm). Thus, a 50% swing about a mean gain of 20 results in swing of 5% about the optimal width of the energy-buildup layer. This robustness feature of the optimization is more clearly

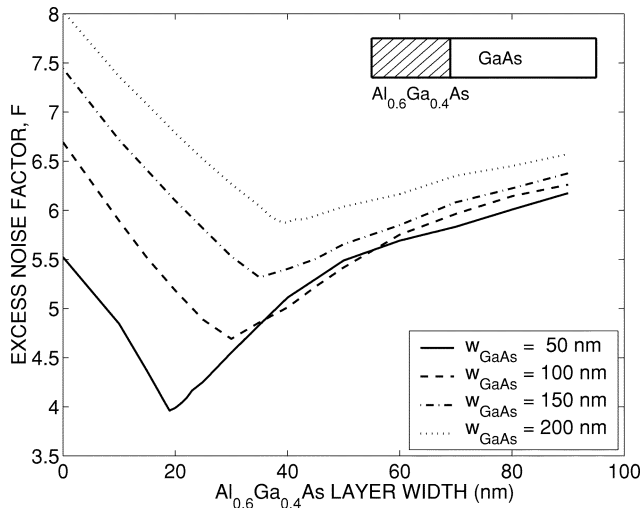


Fig. 6. Excess noise factor F as a function of the width of the energy-buildup layer ($\text{Al}_{0.6}\text{Ga}_{0.4}\text{As}$) for different multiplication-layer widths for a mean gain of 20. Note that each multiplication-layer width has its own optimal energy-buildup-layer width.

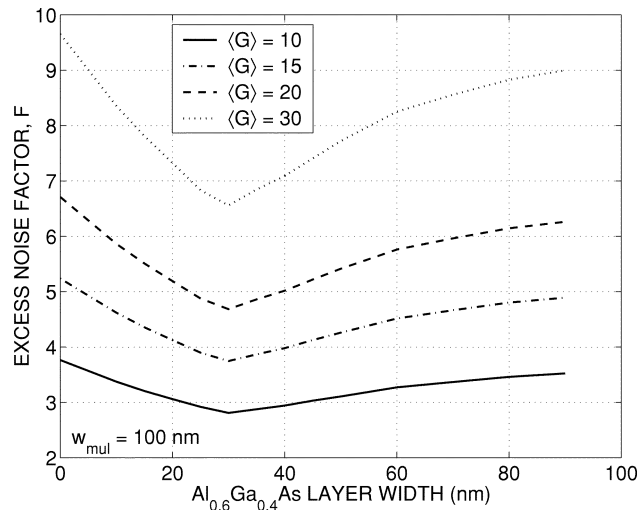


Fig. 7. Excess noise factor F as a function of the width of the energy-buildup layer ($\text{Al}_{0.6}\text{Ga}_{0.4}\text{As}$) parameterized by the mean gain, $\langle G \rangle$. The multiplication-layer width is fixed at 100 nm. Note that the least excess noise factor is observed at the same energy-buildup layer width (29 nm) almost independently of the mean gain.

shown in Fig. 7, where the excess noise factor is plotted as a function of the width of the energy-buildup layer for various mean gain scenarios. Note that the least excess noise factor is always achieved approximately at an energy-buildup-layer width of 29 nm, almost regardless of the gain. This is a remarkable feature from a design perspective, which implies that the excess-noise-factor optimization is achieved *uniformly* in the mean gain.

Moreover, if we compare the optimal excess noise factor in the heterostructure device to the excess noise factor in a homojunction device (with the same multiplication-region width), we see that the reduction in the excess noise factor rendered by the heterostructure becomes more significant as the mean gain increases. This result is shown in Fig. 8, where the *excess-noise-factor improvement*, defined as the net reduction in

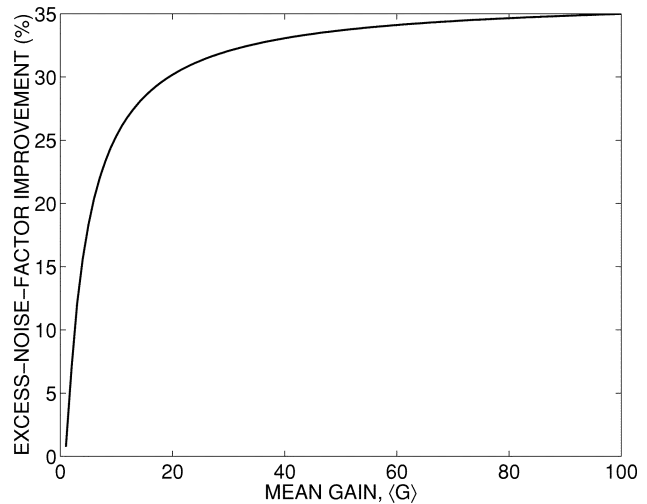


Fig. 8. Percentage excess-noise-factor improvement, as a function of the mean gain, in the optimal heterostructure APD relative to a homojunction APD (without the initial-energy effect).

the excess noise factor relative to the zero-initial energy case, is plotted as a function of the mean gain. This behavior is attributable to two factors. First, we observe that a milder increase in the electric field is required for a device whose injected carriers possess an initial energy than that required to cause a similar gain increase in a device that does not exhibit any initial energy. [This observation is supported by the mean gain vs. electric field curves shown in Fig. 10(b) and (d)]. Thus, as the gain increases for both devices, the dead spaces in the device with the initial energy are longer than the dead spaces associated with the device without the initial energy. Clearly, the device with longer dead space (i.e., the one whose injected carriers have an initial energy) will enjoy a more significant reduction in the excess noise. Second, as the field increases in the device that exhibits the initial-energy effect, its *initial* dead space becomes progressively smaller and the pdf of the distance to the first ionization (for the injected electron) becomes more “impulse-like.” This effect enhances the initial-energy effect as it causes it to more closely resemble the ideal case where the first ionization occurs at the edge of the multiplication region, for which the excess-noise improvement attains its highest value of 0.75¹. In the example considered in Fig. 8, the asymptotic excess-noise-factor improvement is approximately 0.35, however. The reason for not achieving the maximal 0.75 excess-noise-factor improvement is due to the fact that even when the initial dead space is zero (i.e., at very high fields), the pdf will still have a finite spread. One would therefore conclude from this result that the use of an optimized heterostructure APD becomes more important in high-bandwidth applications (e.g., high-speed receivers) where Johnson noise is dominant and high operational gains (as much as the bandwidth constraint permits) are needed to overcome the noise.

¹The maximal excess-noise improvement can be established as follows. Let $F_c(\langle G \rangle)$ denote the excess noise factor for an idealized device for which the first impact ionization occurs instantaneously at the edge of the multiplication layer. Then, according to [17], $[F(\langle G \rangle) - F_c(\langle G \rangle)]/F_c(\langle G \rangle) = 1 - ((1 + F_c(\langle G \rangle)/2)/2 F_c(\langle G \rangle))$, which converges to 0.75 as $\langle G \rangle \rightarrow \infty$ since F_c increases linearly with $\langle G \rangle$ for large $\langle G \rangle$.

Finally, let us now compare the above noise reduction results to the maximal noise reduction in a 200-nm GaAs homojunction which would result from the initial-energy effect (i.e., without the use of an energy-buildup layer). This will show how well the energy-buildup layer in a heterostructure APD is capable to mimic the maximal initial-energy effect in homojunction APDs. Our calculations show that for a 200-nm GaAs homojunction device with zero initial energy, the excess noise factor is 8 (at a gain of 20), and it is 5.4 when the initial energy is equal to the ionization threshold energy (corresponding to a maximal initial-energy effect). Now, by introducing the energy-buildup layer in the proposed heterostructure device, the minimal predicted excess noise factor is 5.8, which occurs at $w_b = 40$ nm. Hence, in this example, the optimized proposed heterostructure is within 8% of the absolute minimum noise attainable using the initial-energy effect. This difference may be a result of residual hole multiplication events in the energy-buildup layer.

B. Sensitivity to Uncertainty in the Initial Energy of Injected Carriers

In Fig. 6, it was assumed that carriers entering the $\text{Al}_{0.6}\text{Ga}_{0.4}\text{As}$ energy-buildup layer had zero initial energy. However, it is important to address the noise behavior in the presence of uncertainty in the initial energy. Fig. 9 shows the excess noise factor as a function of the $\text{Al}_{0.6}\text{Ga}_{0.4}\text{As}$ energy-buildup-layer width for the case when the GaAs multiplication width is 100 nm (at a mean gain of 20) for various initial energy scenarios. As seen in the figure, overall, the excess noise factor is reduced even more in the presence of the initial energy. More importantly, the optimum configuration for the minimal excess noise factor depends upon the initial energy of carriers entering the $\text{Al}_{0.6}\text{Ga}_{0.4}\text{As}$ energy-buildup layer. For example, if injected carriers have zero initial energy, then the minimal excess noise factor ($F = 4.68$) occurs at $w_b = 29$ nm. On the other hand, if carriers have initial energy equivalent to 50% of the ionization threshold energy, then the minimal excess noise factor ($F = 4.26$) occurs at when $w_b = 15$ nm. In addition to minimizing noise, the optimal width renders the added advantage that its associated excess noise factor is least sensitive to uncertainty in the initial energy. This can be seen from Fig. 9, in which the uncertainty in the excess noise factor ΔF , defined as the maximum vertical swing in F as E_{ini} varies between 0 and $E_{\text{th,GaAs}}$ (i.e., the vertical distance between the top and bottom solid curves in Fig. 9), is clearly at a minimum at the optimal width of $w_b = 29$ nm. The point we are making is that the device configuration that results in the least excess noise factor *assuming no initial energy* also exhibits the least excess-noise uncertainty (due to the unknown amount of initial energy). Hence, from a design perspective, it is more robust to optimize the the proposed structure assuming zero initial energy (for carriers entering the $\text{Al}_{0.6}\text{Ga}_{0.4}\text{As}$ layer).

Finally, we examine the dependence of the mean gain and the excess noise factor on the initial energy of injected carriers in an optimized heterostructure. The excess noise factors are shown in Fig. 10 for a 100-nm GaAs homojunction APD [Fig. 10(a)] and a 30-nm $\text{Al}_{0.6}\text{Ga}_{0.4}\text{As}$ energy-buildup layer with a 100-nm GaAs multiplication layer [Fig. 10(c)]. The latter is calculated twice: once with a maximal initial energy (solid curve) and once

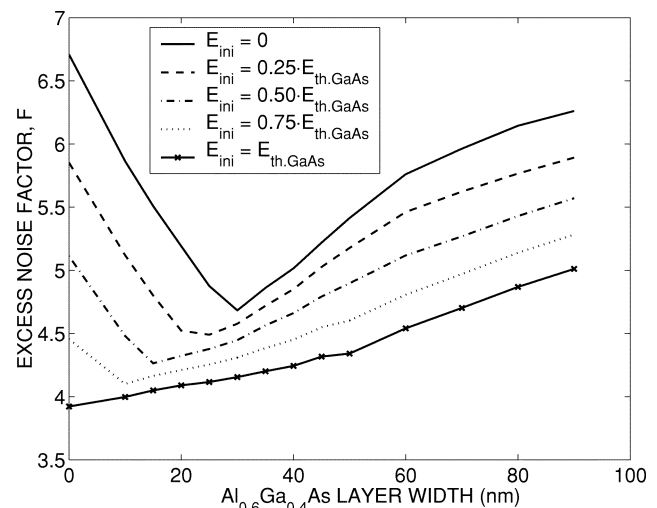


Fig. 9. Sensitivity of the excess noise factor, F , to uncertainty in the initial energy of the injected carriers, as a function of the width of the energy-buildup layer. The GaAs multiplication-layer width is 100 nm and the mean gain is 20. The plots are parameterized by different initial-energy levels for carriers that are injected into the $\text{Al}_{0.6}\text{Ga}_{0.4}\text{As}$ layer.

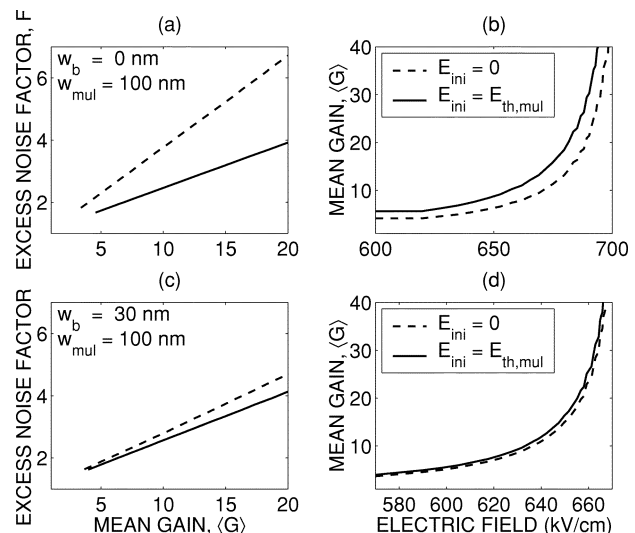


Fig. 10. Excess noise factor as a function of mean gain (left) and the mean gain as a function of the applied electric field (right). (a) and (b) correspond to a 100-nm GaAs homojunction APD while (c) and (d) correspond to a heterostructure APD with a 30-nm $\text{Al}_{0.6}\text{Ga}_{0.4}\text{As}$ energy-buildup layer. Solid curves represent the full initial-energy scenario and dashed curves correspond to the case where the initial energy is zero.

without any initial energy (dashed curve). As seen from the plots, the uncertainty in the excess noise factor, ΔF , is significant for a homojunction APD but relatively small in an optimally designed heterostructure APD. In addition, the fluctuations in the mean gain (due to uncertainty in the initial energy) is large in a homojunction APD and small in an optimally designed heterostructure, as seen from Fig. 10(b) and (d). For example, if a homojunction APD is assumed to have zero initial energy, then the electric field required to produce a mean gain of 20 is approximately 690 kV/cm. However, due to uncertainty in the initial energy, the mean gain with the same electric field may increase to 30, resulting in a 50% mean-gain fluctuation. In contrast, this gain uncertainty in the optimally designed heterostructure APD is only 10%.

IV. CONCLUSIONS

In this paper, we used the newly developed modified dead-space multiplication theory to optimize the design of APDs with two-layer heterostructure multiplication regions. The key mechanism exploited here is the initial-energy effect, which arises from the finite initial energy that carriers possess as they are injected into the multiplication region. This initial energy serves to reduce the first dead space in the avalanche process, which serves to enhance the probability of the first ionization being in the locality of the edge of the multiplication region. The initial-energy effect, or equivalently, the dead-space reduction in the first impact ionization of injected carriers, has been previously shown, both theoretically and experimentally, to reduce the excess noise factor below the limits customarily known for thin APDs.

To exploit this effect in a practical design, we proposed a two-layer $\text{Al}_{0.6}\text{Ga}_{0.4}\text{As}$ -GaAs multiplication-region structure for which an intrinsic $\text{Al}_{0.6}\text{Ga}_{0.4}\text{As}$ layer, called the energy-buildup layer, is used primarily to energize the injected carriers while the intrinsic GaAs layer is used to host the ionization events. In effect, the initial-energy mechanism is naturally brought about in the proposed heterostructure without requiring any initial energy for the carriers that are injected into the $\text{Al}_{0.6}\text{Ga}_{0.4}\text{As}$ layer, a task which would be difficult to enforce in fabrication. It is shown that there is an optimum width of the energy-buildup layer for which the excess noise factor is minimized almost independently of the operational gain. Moreover, such a noise improvement, relative to a homostructure in the absence of the initial-energy effect, becomes more significant at high operational mean gains. Notably, the predicted noise reduction for the optimized structure is very close to that corresponding to the maximal initial-energy effect in homojunction APDs. Moreover, based on the noise reduction seen in this paper, it would be conceivable to consider devices with several stages of two-layer multiplication regions.

The analysis presented here used an idealized model for the dead-space effect for which carriers abruptly become capable of impact ionizing after traveling the field- and material-dependent (but otherwise deterministic) dead space. However, we caution the reader that some of these assumptions may not be very accurate under very high electric-field conditions. In a more realistic setting (especially for very thin structures where the operational electric fields are high), a soft-threshold ionization model should be used for which newly created carriers gradually attain their ionization capability [26]. Moreover, as the amount of energy that a carrier may assume immediately after ionization is random, the dead space itself may be random. The combination of these to nonidealized effects results in a free-path distance pdf that is deviant from the simplified shifted exponential function that we assume in the hard-threshold model. However, in this paper we chose to use the simplified hard-threshold dead-space model as a convenient approximation, which manages to capture the dead-space and initial-energy effects while keeping the mathematical complexity of the model at a minimum. Another approximation adopted here was to neglect the phonon scattering effect in the doped region preceding the energy-buildup layer where the initial energy is accumulated. In

an earlier work, phonon losses were estimated and subtracted from the initial energy, which in turn caused a slight increase in the predicted excess noise factors [17].

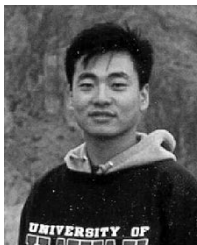
ACKNOWLEDGMENT

The authors wish to thank Dr. J. P. R. David and Dr. G. J. Rees at the University of Sheffield (U.K.) for many valuable discussions and suggestions.

REFERENCES

- [1] P. Yuan, S. Wang, X. Sun, X. G. Zheng, A. L. Holmes, Jr., and J. C. Campbell, "Avalanche photodiodes with an impact-ionization-engineered multiplication region," *IEEE Photon. Technol. Lett.*, vol. 12, pp. 1370–1372, 2000.
- [2] S. Wang, R. Sidhu, X. G. Zheng, X. Li, X. Sun, A. L. Holmes, Jr., and J. C. Campbell, "Low-noise avalanche photodiodes with graded impact-ionization-engineered multiplication region," *IEEE Photon. Technol. Lett.*, vol. 13, pp. 1346–1348, 2001.
- [3] B. E. A. Saleh, M. M. Hayat, and M. C. Teich, "Effect of dead space on the excess noise factor and time response of avalanche photodiodes," *IEEE Trans. Electron Devices*, vol. 37, pp. 1976–1984, 1990.
- [4] M. M. Hayat, B. E. A. Saleh, and M. C. Teich, "Effect of dead space on gain and noise of double-carrier-multiplication avalanche photodiodes," *IEEE Trans. Electron Devices*, vol. 39, pp. 546–552, 1992.
- [5] M. M. Hayat, W. L. Sargeant, and B. E. A. Saleh, "Effect of dead space on gain and noise in Si and GaAs avalanche photodiodes," *IEEE J. Quantum Electron.*, vol. 28, pp. 1360–1365, 1992.
- [6] X. Li, X. Zheng, S. Wang, F. Ma, and J. C. Campbell, "Calculation of gain and noise with dead space for GaAs and $\text{Al}_x\text{Ga}_{1-x}\text{As}$ avalanche photodiode," *IEEE Trans. Electron Devices*, vol. 49, pp. 1112–1117, July 2002.
- [7] P. Yuan, C. C. Hansing, K. A. Anselm, C. V. Lenox, H. Nie, A. L. Holmes, Jr., B. G. Streetman, and J. C. Campbell, "Impact ionization characteristics of III–V semiconductors for a wide range of multiplication region thicknesses," *IEEE J. Quantum Electron.*, vol. 36, pp. 198–204, 2000.
- [8] M. A. Saleh, M. M. Hayat, P. Sotirelis, A. L. Holmes, Jr., J. C. Campbell, B. E. A. Saleh, and M. C. Teich, "Impact-ionization and noise characteristics of thin III–V avalanche photodiodes," *IEEE Trans. Electron Devices*, vol. 48, pp. 2722–2731, 2001.
- [9] M. A. Saleh, M. M. Hayat, O.-H. Kwon, A. L. Holmes, Jr., J. C. Campbell, B. E. A. Saleh, and M. C. Teich, "Breakdown voltage in thin III–V avalanche photodiodes," *Appl. Phys. Lett.*, vol. 79, pp. 4037–4039, 2001.
- [10] M. A. Saleh, M. M. Hayat, B. E. A. Saleh, and M. C. Teich, "Dead-space-based theory correctly predicts excess noise factor for thin GaAs and AlGaAs avalanche photodiodes," *IEEE Trans. Electron Devices*, vol. 47, pp. 625–633, 2000.
- [11] P. Yuan, K. A. Anselm, C. Hu, H. Nie, C. Lenox, A. L. Holmes, Jr., B. G. Streetman, J. C. Campbell, and R. J. McIntyre, "A new look at impact ionization—Part II: Gain and noise in short avalanche photodiodes," *IEEE Trans. Electron Devices*, vol. 46, pp. 1632–1639, 1999.
- [12] K. F. Li, D. S. Ong, J. P. R. David, G. J. Rees, R. C. Tozer, P. N. Robson, and R. Grey, "Avalanche multiplication noise characteristics in thin GaAs p^+i-n^+ diodes," *IEEE Trans. Electron Devices*, vol. 45, pp. 2102–2107, 1998.
- [13] D. S. Ong, K. F. Li, G. J. Rees, G. M. Dunn, J. P. R. David, and P. N. Robson, "A Monte Carlo investigation of multiplication noise in thin p^+i-n^+ GaAs avalanche photodiodes," *IEEE Trans. Electron Devices*, vol. 45, pp. 1804–1810, 1998.
- [14] S. A. Plimmer, J. P. R. David, R. Grey, and G. J. Rees, "Avalanche multiplication in $\text{Al}_x\text{Ga}_{1-x}\text{As}$ ($x = 0$ to 0.60)," *IEEE Trans. Elec. Dev.*, vol. 47, pp. 1089–1097, 2000.
- [15] A. Spinelli, A. Pacelli, and A. L. Lacaita, "Dead space approximation for impact ionization in silicon," *Appl. Phys. Lett.*, vol. 69, pp. 3707–3709, 1996.
- [16] R. J. McIntyre, "A new look at impact ionization—Part I: A theory of gain, noise, breakdown probability, and frequency response," *IEEE Trans. Electron Devices*, vol. 46, pp. 1623–1631, 1999.
- [17] M. M. Hayat, O.-H. Kwon, S. Wang, J. C. Campbell, B. E. A. Saleh, and M. C. Teich, "Boundary effects on multiplication noise in thin heterostructure avalanche photodiodes," *IEEE Trans. Electron Devices*, vol. 49, pp. 2114–2123, Dec. 2002.

- [18] S. Wang, F. Ma, X. Li, R. Sidhu, X. Zheng, X. Sun, A. L. Holmes, Jr., and J. C. Campbell, "Ultra-low noise avalanche photodiodes with a "Centered-Well" multiplication region," *IEEE J. Quantum Electron.*, vol. 39, pp. 375–378, Feb. 2003.
- [19] F. Ma, S. Wang, X. Li, A. Anselm, X. G. Zheng, A. L. Holmes, Jr., and J. C. Campbell, "Monte Carlo simulation of low-noise avalanche photodiodes with heterojunctions," *J. Appl. Phys.*, vol. 92, pp. 4791–4795, Oct. 2002.
- [20] O.-H. Kwon, M. M. Hayat, S. Wang, J. C. Campbell, B. E. A. Saleh, and M. C. Teich, "On the optimization of heterostructure avalanche photodiodes," *IEEE/LEOS Ann. Mtg. Conf. Proc.*, vol. II, pp. 492–493, 2002.
- [21] D. C. Herbert, C. J. Williams, and M. Jaros, "Impact ionization and noise in SiGe multiquantum well structures," *Electron. Lett.*, vol. 32, pp. 1616–1618, Aug. 1996.
- [22] S. A. Plimmer, C. H. Tan, J. P. R. David, R. Grey, K. F. Li, and G. J. Rees, "The effect of an electric-field gradient on avalanche noise," *Appl. Phys. Letts.*, vol. 75, pp. 2963–2965, Nov. 1999.
- [23] G. F. Williams, F. Cappaso, and W. T. Tsang, "The graded bandgap multilayer avalanche photodiode: A new low-noise detector," *IEEE Electron Device Lett.*, vol. EDL-3, pp. 71–73, 1982.
- [24] I. K. Czajkowski, J. Allam, and A. R. Adams, "Role of satellite valleys in ionization rate enhancement in multiple quantum well avalanche photodiodes," *Electron. Lett.*, vol. 26, pp. 1311–1313, Aug. 1990.
- [25] C. K. Chia, J. P. R. David, S. A. Plimmer, G. J. Rees, R. Grey, and P. N. Robson, "Avalanche multiplication in submicron $\text{Al}_x\text{Ga}_{1-x}\text{As}$ /GaAs multilayer structures," *J. Appl. Phys.*, vol. 88, pp. 2601–2608, 2000.
- [26] C. H. Tan, J. P. R. David, G. J. Rees, and R. C. Tozer, "Treatment of soft threshold in impact ionization," *J. Appl. Phys.*, vol. 90, pp. 2538–2543, 2001.



Oh-Hyun Kwon was born in Seoul, Korea, in 1968. He received the B.S. degree in physics in 1995 from the University of the Hawaii, Manoa, and the M.S. degree in electro-optics from the University of Dayton, Dayton, OH. He is currently working toward the Ph.D. degree in electrical and computer engineering at the University of New Mexico, Albuquerque.

His research interests include modeling and fabrication of optoelectronic devices, with emphasis on avalanche photodiodes and quantum-dot infrared

detectors.



Majeed M. Hayat (S'89–M'92–SM'00) was born in Kuwait in 1963. He received the B.S. degree (*summa cum laude*) in electrical engineering from the University of the Pacific, Stockton, CA, in 1985 and the M.S. and Ph.D. degrees in electrical and computer engineering in 1988 and 1992, respectively, from the University of Wisconsin-Madison.

From 1993 to 1996, he was with the University of Wisconsin-Madison as a Research Associate and Co-Principal Investigator for a project on statistical minefield modeling and detection, which was funded by the Office of Naval Research. In 1996, he joined the faculty of the Electro-Optics Graduate Program and the Department of Electrical and Computer Engineering, University of Dayton, Dayton, OH. He is currently an Associate Professor in the Department of Electrical and Computer Engineering, University of New Mexico, Albuquerque. His research interests include modeling and design of high-performance photodetectors, optical communication systems, statistical communication theory, communication networks, infrared imaging and sensors, and statistical signal and image processing.

Dr. Hayat is a recipient of a 1998 National Science Foundation Early Faculty Career Award. He is a member of SPIE and OSA.



Shuling Wang received the B.S. degree in microelectronics from Beijing University, Beijing, China, in 1995, the M.S.E.E. degree from the University of Notre Dame, Notre Dame, IN, in 1999, and the Ph.D. degree from the University of Texas at Austin in August 2002.

She is currently a post-doctorate Researcher in the Microelectronics Research Center, University of Texas at Austin, working on high-speed, low-noise avalanche photodiodes.



Joe C. Campbell (S'73–M'74–SM'88–F'90) received the B.S. degree in Physics from The University of Texas at Austin in 1969, and the M.S. and Ph.D. degrees in physics from the University of Illinois at Urbana-Champaign in 1971 and 1973, respectively.

From 1974 to 1976, he was with Texas Instruments, where he worked on integrated optics. In 1976, he joined the staff of AT&T Bell Laboratories, Holmdel, NJ, where in the Crawford Hill Laboratory he worked on a variety of opto-electronic devices including semiconductor lasers, optical modulators, waveguide switches, photonic integrated circuits, and photodetectors with emphasis on high-speed avalanche photodiodes for high-bit-rate light wave systems. In January 1989, he joined the faculty of The University of Texas at Austin as a Professor of Electrical and Computer Engineering and Cockrell Family Regents Chair in Engineering. At present, he is actively involved in Si-based optoelectronics and high-speed photodiodes. He has coauthored six book chapters, more than 200 journal publications, and 130 conference presentations.

In 2002, he was elected into the National Academy of Engineering.



Archie Holmes, Jr. (M'92) received the B.S.E.E. degree from The University of Texas at Austin in 1991 and the M.S. and Ph.D. degrees in electrical engineering from the University of California, Santa Barbara, in 1992 and 1997, respectively.

He joined the Department of Electrical and Computer Engineering of The University of Texas at Austin as an Assistant Professor in 1997. His major research areas are in electronic materials and devices, including growth of novel semiconductor alloys by molecular beam epitaxy, high-speed photodetectors, and heterogeneous materials integration via direct wafer bonding. He has published more than 80 journal and conference papers.

Dr. Holmes is a member of IEEE Lasers and Electro-Optics Society and the American Society for Engineering Education.



Yi Pan (S'91–SM'91) received the B.Eng. and M. Eng. degrees in computer engineering from Tsinghua University, Tsinghua, China, in 1982 and 1984, respectively, and the Ph.D. degree in computer science from the University of Pittsburgh, Pittsburgh, PA, in 1991.

Currently, he is an Associate Professor in the Department of Computer Science, Georgia State University, Atlanta. His research interests include parallel and distributed computing, optical networks, wireless networks, and bioinformatics. His pioneer work on computing using reconfigurable optical buses has inspired extensive subsequent work by many researchers, and his research results have been cited by more than 100 researchers worldwide in books, theses, journal and conference papers. He is a co-inventor of three U.S. patents (pending) and five provisional patents. He has co-edited nine books/proceedings and published more than 130 research papers including over 60 journal papers (more than 20 of which have been published in various IEEE journals). He has served as a reviewer/panelist for many research foundations/agencies such as the U.S. National Science Foundation, the Natural Sciences and Engineering Research Council of Canada, the Australian Research Council, and the Hong Kong Research Grants Council. He has delivered over 40 invited talks, including keynote speeches and colloquium talks, at conferences and universities worldwide. His recent research has been supported by the NSF, NIH, AFOSR, AFRL, JSPS, and the states of Georgia and Ohio.

Dr. Pan has served as an Editor-in-Chief or Editorial Board Member for eight journals, including three IEEE TRANSACTIONS, and a Guest Editor for seven special issues. He has organized several international conferences and workshops and has also served as a Program Committee Member for several major international conferences, such as INFOCOM, GLOBECOM, ICC, IPDPS, and ICPP. He is an IEEE Distinguished Speaker (2000–2002), a Yamacraw Distinguished Speaker (2002), and a Shell Oil Colloquium Speaker (2002). He has received many awards from agencies such as the NSF, AFOSR, JSPS, IISF and Mellon Foundation. He is listed in *Men of Achievement*, *Who's Who in the Midwest*, *Who's Who in America*, and *Who's Who in American Education*.



Bahaa E. A. Saleh (M'73–SM'86–F'91) received the B.S. degree from Cairo University, Cairo, Egypt, in 1966 and the Ph.D. degree from The Johns Hopkins University, Baltimore, MD, in 1971, both in electrical engineering.

He has been a Professor and Chairman of the Department of Electrical and Computer Engineering, Boston University, Boston, MA, since 1994. He is also Deputy Director of the National Science Foundation (NSF) Center for Subsurface Sensing and Imaging Systems, an NSF Engineering Research

Center, a Co-Director of the Quantum Imaging Laboratory, and a member of the Boston University Photonics Center. He held faculty and research positions at the University of Santa Catarina in Brazil, Kuwait University, Max Planck Institute in Germany, the University of California-Berkeley, the European Molecular Biology Laboratory, Columbia University, and the University of Wisconsin-Madison, where he was a faculty member from 1977 to 1994, and served as Chairman of the Department of Electrical and Computer Engineering from 1990 to 1994.

His research contributions cover a broad spectrum of topics in optics and photonics including statistical and quantum optics, optical communication and signal processing, nonlinear optics, photodetectors, digital image processing, and vision. He is the author of two books, *Photoelectron Statistics* (New York: Springer-Verlag, 1978) and (with M. C. Teich) *Fundamentals of Photonics* (New York: Wiley-InterScience, 1991), chapters in seven books, and more than 180 papers in technical journals.

Dr. Saleh served as Editor-in-Chief of the *Journal of the Optical Society of America A* from 1991 to 1997, and is presently the Chairman of the Board of Editors of the Optical Society of America. He is the recipient of the 1999 Optical Society of America Esther Hoffman Beller Award for outstanding contributions to optical science and engineering education. He is a Fellow of the Optical Society of America and the Guggenheim Foundation and a member of Phi Beta Kappa, Sigma Xi, and Tau Beta Pi.



Malvin C. Teich (S'62–M'66–SM'72–F'89) received the B.S. degree in physics from the Massachusetts Institute of Technology (MIT), Cambridge, the M.S. degree in electrical engineering from Stanford University, Stanford, CA, and the Ph.D. degree from Cornell University, Ithaca, NY.

His first professional association, in 1966, was with MIT Lincoln Laboratory, Lexington, MA. He joined the faculty at Columbia University, New York, in 1967, where he served as a member of the Electrical Engineering Department (as Chairman from 1978 to 1980), the Applied Physics Department, and the Columbia Radiation Laboratory. During his tenure at Columbia, he carried out extensive research in the areas of noise in avalanche photodiodes and fiber-optic amplifiers, photon statistics and point processes, and the generation of squeezed light. In 1996, he was appointed Professor Emeritus of Engineering Science and Applied Physics at Columbia University. He has been teaching and pursuing his research interests at Boston University, Boston, MA, as a faculty member, with joint appointments in the Departments of Electrical and Computer Engineering, Physics, and Biomedical Engineering since 1995. He is a Member of the Quantum Imaging Laboratory, the Photonics Center, and the Center for Adaptive Systems and also serves as a consultant to government and private industry. He is most widely known for his work in photonics and quantum optics. His current efforts in photonics are associated with the reduction of noise in avalanche photodiodes and fiber-optic amplifiers; his efforts in quantum optics are directed toward developing imaging systems that make use of the correlation properties of entangled photon pairs generated in nonlinear optical parametric downconversion. He has authored or coauthored some 300 technical publications and holds two patents. He is the coauthor of *Fundamentals of Photonics* (New York: Wiley, 1991).

Dr. Teich has served as a member of the Editorial Advisory Panel for the journal *Optics Letters* from 1977 to 1979, as a Member of the Editorial Board of the *Journal of Visual Communication and Image Representation* from 1989 to 1992, and as Deputy Editor of *Quantum Optics* from 1988 to 1994. He is currently a Member of the Editorial Board of the journal *Jemná Mechanika a Optika* and a Member of the Advisory Board of the IEEE Press Series *Emerging Technologies in Biomedical Engineering*. In 1969, he received the IEEE Browder J. Thompson Memorial Prize for his paper "Infrared Heterodyne Detection." He was awarded a Guggenheim Fellowship in 1973. In 1992, he was honored with the Memorial Gold Medal of Palacký University, Czech Republic, and in 1997 he was the recipient of the IEEE Morris E. Leeds Award. He is a Member of the Scientific Board of the Czech Academy of Sciences' Institute of Physics and a Fellow of the Optical Society of America, the American Physical Society, the American Association for the Advancement of Science, and the Acoustical Society of America. He is a member of Sigma Xi and Tau Beta Pi.